Cell, Vol. 99, 81–92, October 1, 1999, Copyright ©1999 by Cell Press

MT1-MMP-Deficient Mice Develop Dwarfism, Osteopenia, Arthritis, and Connective Tissue Disease due to Inadequate Collagen Turnover

Kenn Holmbeck,[1,7] Paolo Bianco,[3,7] John Caterina,[1] Susan Yamada[1] Mark Kromer,[1] Sergei A. Kuznetsov,[2] Mahesh Mankani,[2] Pamela Gehron Robey,[2] A. Robin Poole,[4] Isabelle Pidoux,[4] Jerrold M. Ward[5] and Henning Birkedal-Hansen,[1,6]

[1]MMP Unit
[2]Craniofacial and Skeletal Diseases Branch
National Institute of Dental and Craniofacial Research
Bethesda, Maryland 20892
[3]Universita "La Sapienza"
Rome 00161
and Universita dell'Aquila
L'Aquila 67100
Italy
[4]Joint Diseases Laboratory
Shriners Hospitals for Children
Canadian Unit
McGill University
Montreal, Quebec, H3G 1A6
Canada
[5]Veterinary and Tumor Pathology Section
Animal Sciences Branch
Division of Basic Sciences
National Cancer Institute
Frederick, Maryland 21702–1201

Summary

MT1-MMP is a membrane-bound matrix metalloproteinase (MT-MMP) capable of mediating pericellular proteolysis of extracellular matrix components. MT1-MMP is therefore thought to be an important molecular tool for cellular remodeling of the surrounding matrix. To establish the biological role of this membrane proteinase we generated MT1-MMP-deficient mice by gene targeting. MT1-MMP deficiency causes craniofacial dysmorphism, arthritis, osteopenia, dwarfism, and fibrosis of soft tissues due to ablation of a collagenolytic activity that is essential for modeling of skeletal and extraskeletal connective tissues. Our findings demonstrate the pivotal function of MT1-MMP in connective tissue metabolism, and illustrate that modeling of the soft connective tissue matrix by resident cells is essential for the development and maintenance of the hard tissues of the skeleton.

Introduction

Matrix metalloproteinases (MMPs) constitute a family of zinc endopeptidases that are capable of degrading most of the structural components of the extracellular matrix (Birkedal-Hansen et al., 1993; Birkedal-Hansen, 1995; Werb, 1997). The wide substrate specificity suggests that MMPs play an important role in mediating fundamental cellular programs that depend on stromal remodeling such as cell migration, angiogenesis, and wound healing (Mignatti and Rifkin, 1996; Okada et al., 1997; Nagase, 1998). In addition, MMPs may be important cellular tools in embryonic development, in growth, in mammary involution, and in a number of diseases such as arthritis, atherosclerosis, and cancer (Liotta et al., 1991; Stetler-Stevenson et al., 1993; Galis et al., 1995; Werb et al., 1996; Chin and Werb, 1997; Lark et al., 1997).

While most MMPs are secreted, MT-MMPs, a recently identified subset of MMPs, are membrane-associated (Sato et al., 1994; Takino et al., 1995; Will and Hinzmann, 1995; Puente et al., 1996; Pei, 1999). MT-MMPs are type I membrane proteins with a single transmembrane domain and an extracellular catalytic domain. The membrane localization makes MT-MMPs particularly suited to function in pericellular proteolysis (Sato et al., 1996). MT1-MMP is highly expressed in embryonic skeletal and periskeletal tissues (Kinoh et al., 1996; Apte et al., 1997), and has been suggested to serve as a membrane receptor or activator of MMP-2 (Gelatinase A) and possibly other secreted MMPs (Strongin et al., 1995; Cowell et al., 1998). Recent data indicate that MT1-MMP may also function as a fibrinolytic enzyme in the absence of plasmin and mediate pericellular proteolysis in angiogenesis (Hiraoka et al., 1998).

Mouse strains deficient in several individual MMPs (MMP-2, MMP-3, MMP-7, MMP-9, MMP-12) have been developed. All of these showed little or no impairment of development and reproduction. In each case, however, specific cellular functions were altered or impaired either spontaneously or following defined experimental challenge (Shipley et al., 1996; Itoh et al., 1997; Wilson et al., 1997; Masson et al., 1998; Mudgett et al., 1998; Vu et al., 1998). To address by similar means the physiological role of MT1-MMP, we generated mutant mice deficient in MT1-MMP activity. We demonstrate here that MT1-MMP deficiency gives rise to a set of severe, generalized connective tissue abnormalities by impairing an essential collagenolytic activity.

Results

Generation of MT1-MMP-Deficient Mice

To disrupt expression of the *MT1-MMP* gene, a 3.35 kb segment containing sequences from the 3′ half of intron 1 through the 3′ end of exon 5 was replaced with a PGK controlled HPRT minigene (van der Lugt et al., 1991) (Figure 1A). This deletion removed from the mature MT1-MMP protein amino acid residues 6–274 including all but five residues of the prodomain and eight residues of the catalytic domain, rendering any polypeptide expressed from this mutant gene catalytically inactive. The targeting vector was transfected into (HM-1) HPRT-deficient mouse embryonic stem cells (Magin et al., 1992) and 35 of 71 HAT-resistant cell clones were identified as legitimately targeted. Chimeric offspring derived from two individual cell clones were mated to Swiss Black

[6]To whom correspondence should be addressed (e-mail: hbhansen@dir.nidcr.nih.gov).
[7]These authors contributed equally.

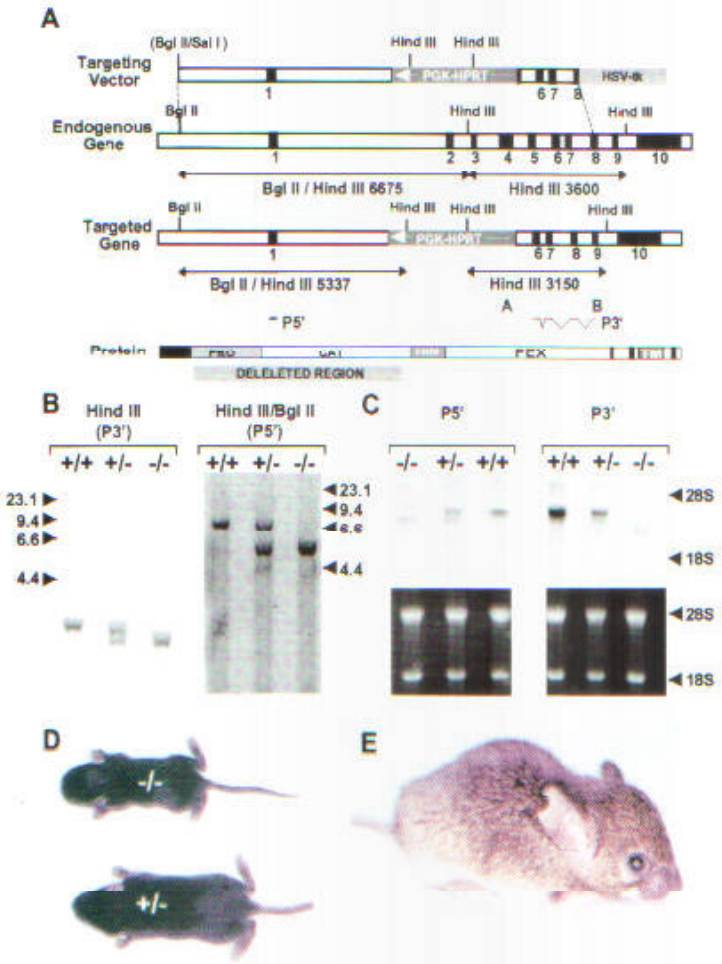

Figure 1. Targeting of MT1-MMP

(A) Strategy for targeting of MT1-MMP. The structure of the mouse *MT1-MMP* endogenous gene, the *MT1-MMP* transgene targeting vector, the targeted *MT1-MMP* gene and the corresponding protein products are depicted as diagrams. In the gene diagram, intron sequences are depicted as open and exon sequences as black boxes. Important restriction sites are indicated. Restriction sites in parenthesis are mutated and not cleavable. The selective markers HPRT and HSV-tk are depicted as shaded boxes. The position of primers used for detection of the targeted allele are indicated with A and B. Probes used for hybridization are indicated as P5′ and P3′. Protein diagram abbreviations are as follows: PRO, prodomain; CAT, catalytic domain; HIN, hinge region; PEX, hemopexin domain; TM, transmembrane domain. "Deleted region" indicates the part of the MT1-MMP protein that is removed by the homologous recombination event.

(B) Identification of transgenic animals by Southern blot: +/−, wild-type; +/−, heterozygous; −/−, homozygous mutant. HindIII-restricted samples were size fractionated and hybridized to the P3′ probe. HindIII/BglII-restricted samples were size fractionated and hybridized to the P5′ probe. The fragment size of the analytical restriction digest is indicated in base pair length and with double arrowhead lines in (A).

(C) Detection of *MT1-MMP* mRNA in total neonate RNA by Northern blot. The genotypes are abbreviated as described for Southern blot. Probes used for detection of fractionated RNA are indicated (P5′ and P3′).

(D) Dorsal view of 10-day-old $MT1^{-/-}$ mouse and control littermate ($MT1^{+/-}$).

(E) Close-up of 79-day-old $MT1^{-/-}$ mouse.

mice and germline transmission of the targeted allele was obtained with chimeras derived from both clones (Figure 1B). Interbreeding of heterozygous mice gave rise to the expected Mendelian distribution of homozygous mutant mice ($MT1^{-/-}$), heterozygous ($MT1^{+/-}$) mice, and wild-type ($MT1^{+/+}$) mice. RNA prepared from total neonatal $MT1^{-/-}$ tissues and probed with exon 1– or exon 6–9–specific probes showed no transcripts of the size or intensity characteristic of *MT1-MMP* mRNA from wild-type or heterozygous littermates (Figure 1C).

MT1-MMP-Deficient Mice Are Viable but Display Severe Runting, Wasting, and Increased Mortality

Neonate MT1-MMP-deficient mice could not be distinguished visibly from heterozygous and wild-type littermates at birth although subsequent X-ray analyses showed evidence of aberrant cranial bone formation already at birth. Hair growth and eye opening occurred without retardation, but growth impairment (smaller body size and weight) became evident as early as 5 days. In cohorts of 30 mice weaning weight for $MT1^{-/-}$ animals ranged from only 3.5 to 5 g versus 12 to 16 g for wild-type or heterozygous mice, and 33% of mutant animals died from wasting before weaning. Surviving mutant mice gained little weight over the next few weeks and after day 50 experienced progressive wasting, patchy hair loss, reduced mobility, kinking of the wrist, and hyperlordosis/hyperkyphosis (Figures 1D and 1E). The mutant mice showed no signs of sexual maturation, and most of the animals died between days 50 and 90. In most, if not all cases, death occurred due to wasting. Heterozygous mice appeared indistinguishable from wild-type littermates. Thus, deleterious effects of any protein translated from the low levels of aberrant size message detected by Northern blot did not account for the observed phenotype in $MT1^{-/-}$ animals.

MT1-MMP Deficiency Causes Skeletal Dysplasia, Arthritis, Severe Osteopenia, and Generalized Soft Tissue Disorders

MT1-MMP deficient mice gradually developed a severe skeletal phenotype (Figures 1D, 1E, and 2). Short snout, orbital protrusions, hypertelorism, and dome-shaped skull with bulging parietal and interparietal regions became obvious at day 5 (Figures 1D and 1E). Membranous ossification of calvarial bones was delayed and suture closure was never completed (Figures 2A and 2C). Beginning at day 5, the limb bones appeared shorter than in control littermates and grew to approximately 65% of the length of controls by day 45 (Figures 2B and

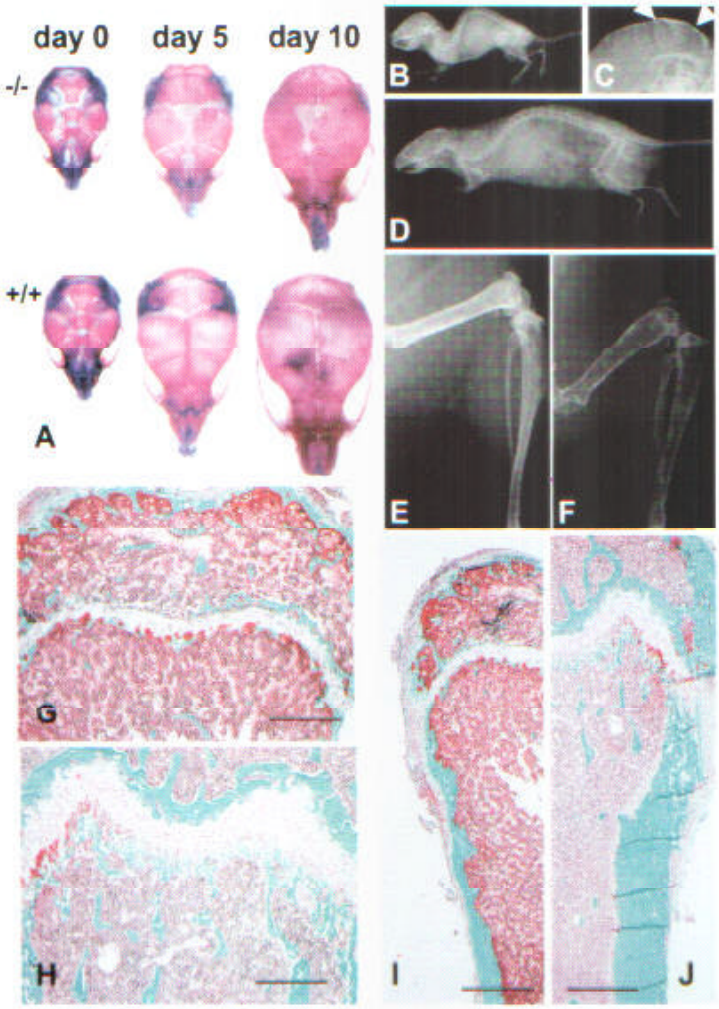

Figure 2. Bone Development in MT1-MMP-Deficient Mice

(A) Alizarin red/alcian blue staining of skulls of MT1-MMP-deficient (−/−) and control (+/+) mice demonstrating larger fontanelles and gradually increasing cranial dysmorphism of mutant mice (3× magnification).

(B–D) Lateral X-ray images of 80-day-old MT1-MMP-deficient (B) and wild-type littermate (D), (0.75× magnification). (C) 3× magnification of cranial vault from the animal in (B). Note the wide sutures and the displacement of the interparietal bone (arrowheads).

(E and F) X-ray images of hind limb bones from 80-day-old MT1-MMP-deficient (F) (3× magnification) and wild-type littermate (E) (2× magnification). Note the severe osteopenia of the mutant mouse.

(G–J) Histology of the femora of 60-day-old MT1-MMP-deficient (G and I) and wild-type (H and J) mice. Note the severe reduction of trabecular bone in the spongiosa and the thinner cortex in the mutant animal (G–H). Goldner's stain. Bars = 150 μm (G and H); 400 μm (I and J).

2D–2F). Osteopenia became increasingly apparent and bone mass was severely reduced in animals aged 40 days or older (Figures 2G–2J). Concurrently, MT1-MMP-deficient mice developed severe generalized arthritis (Figures 3A–3F). All joints showed overgrowth of a hypercellular, vascularized synovial tissue and destruction of articular cartilage, resulting in ankylosis (Figure 3E). TRAP-positive, osteoclast-like giant cells were prominent within articular and periarticular soft tissues (Figures 3C and 3D). Tendons, ligaments, synovial capsules, musculotendinal junctions, and septal/fascia structures associated with skeletal muscle all displayed increased cell proliferation and vascularity, and became increasingly fibrotic. Older animals developed progressive fibrosis of the dermis and of hair follicles, which coincided with hair loss.

Abnormal Cranial Morphogenesis in *MT1-MMP*$^{-/-}$ Mice: Impaired Removal of Calvarial Cartilage Primordia Interferes with Membranous Bone Formation and Suture Closure

Membranous ossification of the parietal, orbital, and lower frontal regions of the mouse calvarium, which are dysmorphic in MT1-MMP-deficient mice, is preceded by cartilage primordia (Kaufmann, 1998). We identified a distinct anomaly in postnatal development of these primordia in MT1-MMP-deficient mice, which also helped to more clearly define the normal process governing ossification. To our knowledge, this process has not previously been fully described. The postnatal development of the most conspicuous primordium, the parietal cartilage (Chen et al., 1998)—which is located in the region where parietal and interparietal bones later develop—is shown in Figure 4. Toward the base of the cranium, the parietal cartilage merged with the cartilage precursor of the pars petrosa of the temporal bone. In normal mice, the cartilaginous precursor of the pars petrosa, and the parietal cartilage (both clearly detectable in newborn mice) were completely replaced by bone at day 15 (Figures 4A–4D). Upon completion of the process, the osseous pars petrosa and the osseous interparietal/parietal bones were joined by typical sutures. The pars petrosa ossified endochondrally whereas the parietal and interparietal bones ossified intramembranously over the outer aspect of the parietal cartilage. Endochondral ossification of the cartilage precursor of the pars petrosa occurred in timely fashion in both normal and mutant mice but the parietal cartilage was never

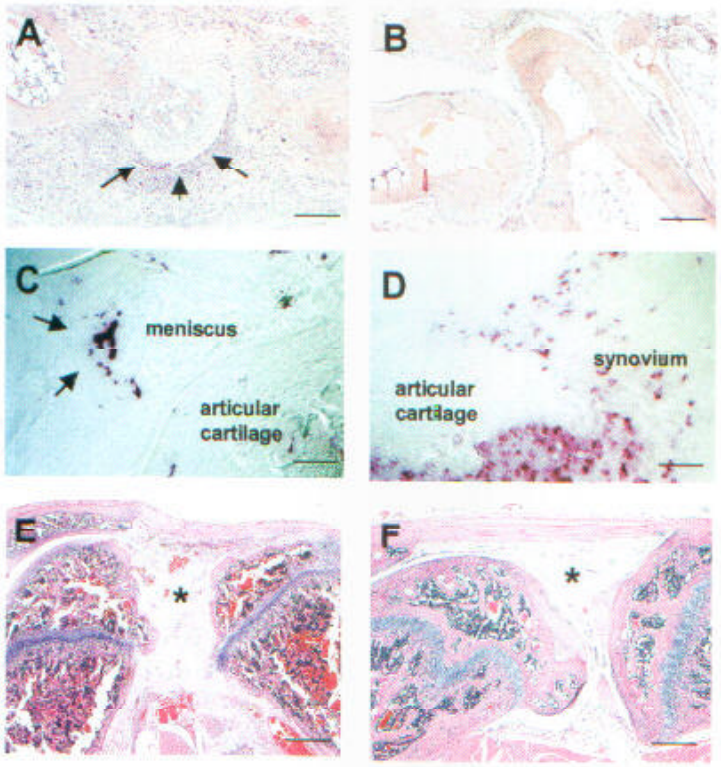

Figure 3. Arthritis in MT1-MMP-Deficient Mice

Metatarsal–phalangeal joint of 40-day-old MT1-MMP-deficient mouse (A), and normal littermate (B). Note the prominent synovitis and the overgrowth of inflamed synovial tissue over the articular cartilage (arrows) in (A). (C and D) Osteoclast-like cells in articular soft tissues of MT1-MMP-deficient mice. (C) TRAP-positive cells at the lateral aspect of a fibrocartilage meniscus in the knee joint. (D) Large numbers of TRAP-positive cells in the synovial overgrowth covering the articular surface of the condyle. (E) Severe ankylosis due to extensive fibrosis of the articular soft tissues in the knee joint of a 103-day-old MT1-MMP-deficient mouse. (F) Control littermate. Asterisks indicate the fibrotic tissue in the mutant mouse and the normal synovial adipose cushion in the wild type. Bars = 200 μm (A and B); 150 μm (C and D); 800 μm (E and F).

removed in MT1-MMP-deficient mice. This primordium persisted but was gradually transformed into an increasingly fibrotic and acellular vestige on the inner aspect of the underdeveloped parietal/interparietal bone at least up to 60 days of age (Figures 4E–4H). The regressing parietal cartilage in normal animals never calcified but gradually dissolved and disappeared by a process that did not involve osteoclasts. We interpret the persistence of the parietal cartilage vestige in MT1-MMP-deficient mice to indicate that a collagenolytic mechanism responsible for dissolution of this cartilage matrix was impaired. This specific chondrolytic process is MT1-MMP-dependent and indispensable for timely removal of cartilage primordia as they are replaced by bone formed by intramembranous ossification.

Endochondral Ossification in *MT1-MMP*$^{-/-}$ Mice: Deficient Vascularization of Hyaline Cartilage Disrupts Secondary Ossification and Growth Plate Development

Maturation, hypertrophy, and calcification of pre- and early postnatal metaphyseal growth plates were essentially normal in mutant mice. In contrast, the postnatal development of the epiphyseal (secondary) ossification centers was markedly delayed. Vascular canals, which normally penetrate the uncalcified hyaline epiphyseal cartilage, did not form. Vascular invasion and subsequent endochondral ossification of the epiphyseal centers normally proceeds from these canals (Figures 5A–5H), and their absence in mutant animals severely retarded secondary ossification. After a delay of about 8 days, the epiphyseal centers of MT1-MMP-deficient mice eventually did ossify, in the absence of vascular canals, but by an alternative mechanism. The endochondral ossification proceeded directly from the perichondrium behind osteoclastic resorption of the calcified cartilage matrix, but only after full expansion of the region of cartilage mineralization to the very periphery of the epiphyses (Figures 5I–5J). Following this delayed development of secondary epiphyseal centers, the metaphyseal growth plates of mutant mice underwent progressive thinning and disorganization (Figures 2G and 2H). BrdU labeling revealed that chondrocyte proliferation was markedly reduced in growth plates of 39-day-old MT1-MMP-deficient mice (Figures 5K and 5L) whereas no such difference was observed at 10 days (not shown).

Increased Osteoclastic Resorption and Decreased Bone Formation are Associated With Progressive Fibrosis of Periskeletal Soft Tissues and Arthritis

The progressive osteopenia observed in adult MT1-MMP-deficient mice was a result of increased bone resorption as well as diminished bone formation. Excessive osteoclastic resorption was observed in all bones of mutant mice aged 40 days or older (Figures 6A–6C). The largest number of osteoclasts was found near bone/soft tissue interfaces: at the bony edges of the open fibrotic cranial sutures, within and near arthritic joints and near tendon, ligament, and capsule insertions of long bones. Dual calcein labeling revealed that bone formation was dramatically reduced in MT1-MMP deficient mice (Figures 6D and 6E). The periosteal osteogenic layer of long bones showed marked fibrosis, reduced cell proliferation (data not shown), and structural disorganization in mice aged 40 days or older (Figures 6F–6I).

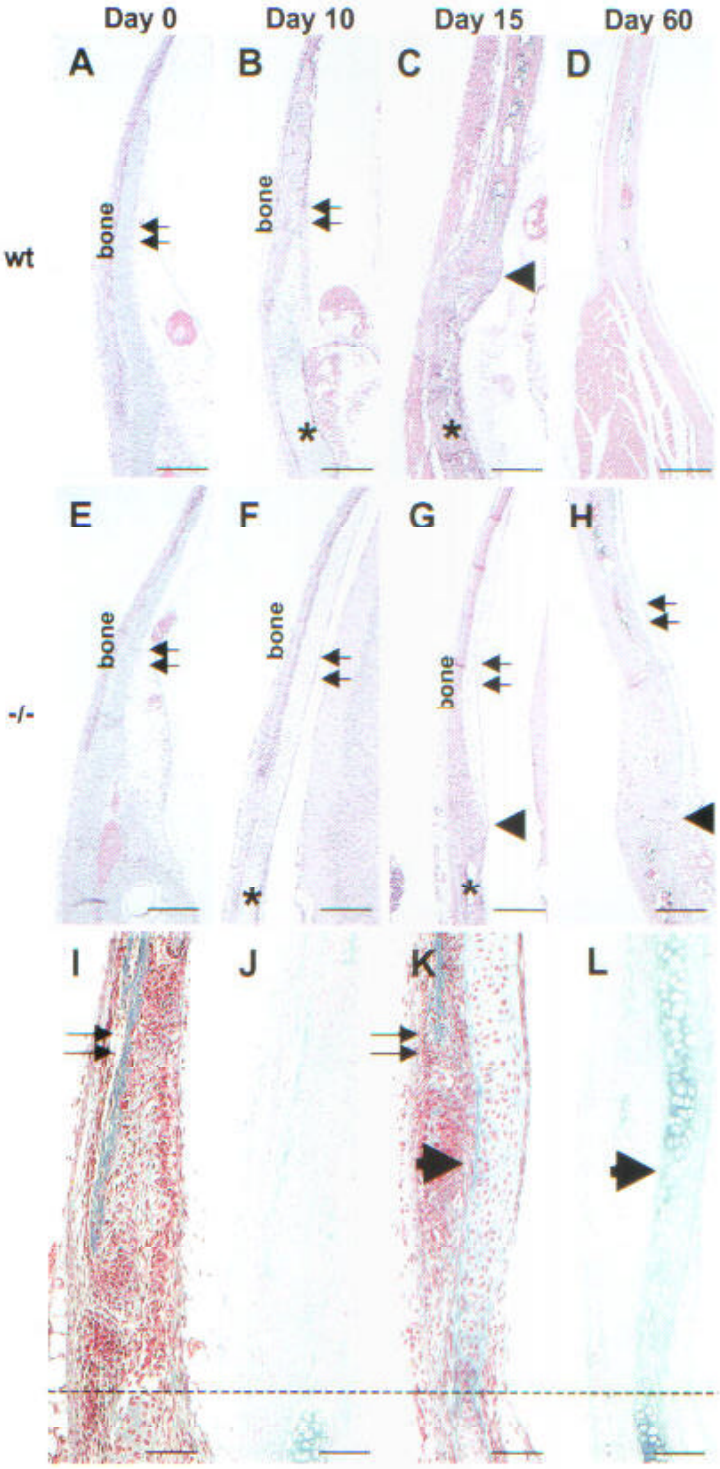

Figure 4. Impaired Chondrolytic Regression of Calvarial Cartilage Primordia in MT1-MMP-Deficient Mice

Coronal sections through the interparietal bones of newborn, 10-, 15-, and 60-day-old normal (A–D) and mutant (E–H) littermates. In newborn mice, the interparietal (and parietal) bones grow on the outside of a cartilage primordium in continuity with the pars petrosa of the temporal bone (A–D). Cartilage hypertrophy is obvious in the pars petrosa at day 10, both in normal and mutant mice (asterisks in B and F). Above the region of cartilage hypertrophy, the parietal cartilage primordium disappears in normal mice, leaving room for the advancing front of membranous ossification ([B], double arrows, and details in [I] and [J]). In mutant mice, a fibrous vestige of the cartilage primordium ([F], double arrows and details in [K], and [L]) contiguous with the hypertrophic cartilage of the pars petrosa ([F], asterisk; [K], thick arrow) remains. At day 15 in normal mice (C), both the pars petrosa (C, asterisk) and the interparietal bone are fully ossified, and joined by a typical suture (C, thick arrow). At day 15 in mutant mice (G) endochondral ossification of the pars petrosa has been completed (G, asterisk), but membranous ossification of the interparietal bone is incomplete, and the vestige of the cartilage primordium persists at its inner aspect (G, double arrow). The lower end of this primordium interferes with suture formation (G, thick arrow). At 60 days, the suture has become highly fibrotic in mutant mice (H, thick arrow) and an acellular fibrous vestige of the primordial cartilage is still detectable (H, double arrows). (I–L) Sections from 10-day-old mice stained with Masson's trichrome (I and K) and alcian blue (J and L). (I and J) normal mice, (K and L) mutant littermates. Thick arrows indicate the unremoved parietal cartilage vestige, which has lost alcianophilia for the most part (L). Thin arrows indicate the forming interparietal bone. The cashed line marks the site of the developing suture, and the boundary between the pars petrosa and the parietal cartilage. Bars = 150 μm (A–H); 70 μm (I–L).

Osteoblasts located at or near bone surfaces were displaced into the dense fibrotic periosteal matrix and frequently showed abundant coarse cytoplasmic inclusions containing collagen fibrils (Figures 6J–6L). Northern blot analysis of total RNA from wild type and mutant mice demonstrated that the expression level of type I and type I' collagen was equivalent in all animals (data not shown). We therefore concluded that excess collagen deposition was unlikely to be caused by increased expression.

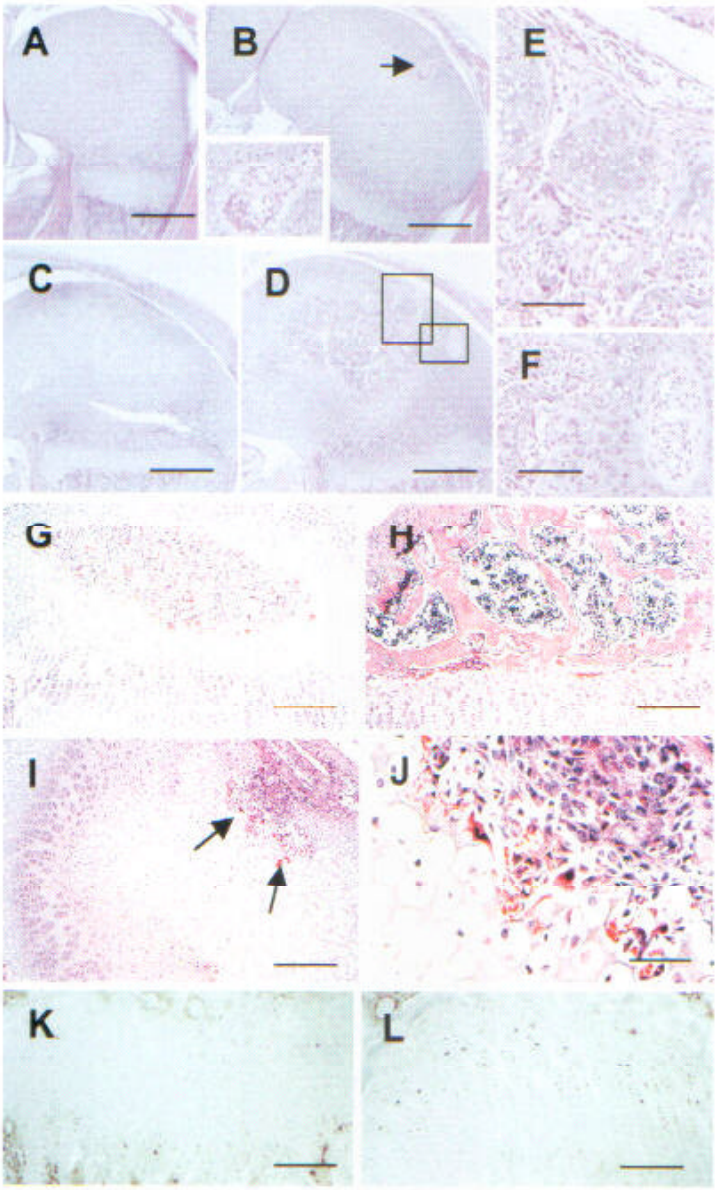

Figure 5. Abnormal Long Bone Development in MT1-MMP-Deficient Mice

(A and B) Femur, 5-day-old mutant and normal mice. Formation of epiphyseal vascular canals within uncalcified epiphyseal cartilage is absent in the mutant mouse (A) and present in the normal littermate (B, arrow and inset). (C and D) Femur, 10-day-old mutant and normal mice. Obvious features of epiphyseal cartilage hypertrophy in the mutant mouse (C). Note the complete absence of vascular canals and of ossification. Ossification of secondary (epiphyseal) center has started in the normal mouse (D). Invasion of the epiphyseal ossification center proceeds from vascular canals (D, boxed, E and F) which penetrate the uncalcified cartilage of the epiphysea. condyle. (G and H) Proximal epiphyses of the tibia of mutant (G) and normal (H) mice, day 16. Ossification of the epiphysis is extensive in the normal mouse, but only beginning in the mutant. (I and J) Femoral epiphysis of 16-day-old mutant mouse. Invasion of the cartilage is led by calcified-cartilage resorbing osteoclasts (I; arrows, J). Osteoclastic resorption of the now mineralized cartilage proceeds without prior development of vascular canals. (K and L) BrdU labeling of the tibial growth plates from 39-day-old mice showing markedly reduced labeling in the mutant (K). Compare to the normal littermate (L). Bars = 300 μm (A–D); 120 μm (E and F); 200 μm (G–I); 70 μm (J); 180 μm (K and L).

MT1-MMP Deficiency Impairs Collagenolytic Activity and Osteogenic Potential of Osteoblasts

Since our findings showed that bone formation was markedly reduced in MT1-MMP deficient animals, we asked whether MT1-MMP deficiency caused an intrinsic dysfunction of osteogenic cells, rather than systemic (e.g., hormonal, nutritional) imbalances, or dysfunction of other skeletal cell types or tissues (for instance vasculature). To answer this question, we isolated clonogenic osteoprogenitor cells (CFU-F) from the bone marrow of mutant mice and normal littermates, and probed their ability to form bone in a transplantation assay (Krebsbach et al., 1997). Cells from mutant mice showed higher colony forming efficiency than cells from normal littermates (data not shown), indicating that CFU-F were not quantitatively deficient in the bone marrow of mutant mice. Culture-expanded populations of marrow-derived osteogenic cells were loaded onto either (denatured) insoluble collagen-type-I-based (Gelfoam) or hydroxyapatite-based carriers and transplanted into the subcutis of immunocompromised, but MT1-MMP-sufficient mice. With both carriers, cells from control mice formed complete ectopic ossicles composed of abundant bone and hematopoietic marrow (Figure 7A). In contrast, cells from mutant littermates formed only scant amounts of bone indicating that the osteogenic activity of marrow-derived osteogenic cells from these animals was severely deficient (Figure 7A). The Gelfoam matrix was efficiently degraded and replaced by bone and marrow in ossicles formed by MT1-MMP-sufficient cells, whereas a significant fraction of the collagenous carrier material remained undegraded in ossicles formed by mutant cells (Figure 7A). We concluded that MT1-MMP-deficient marrow stromal cells possess two seemingly related

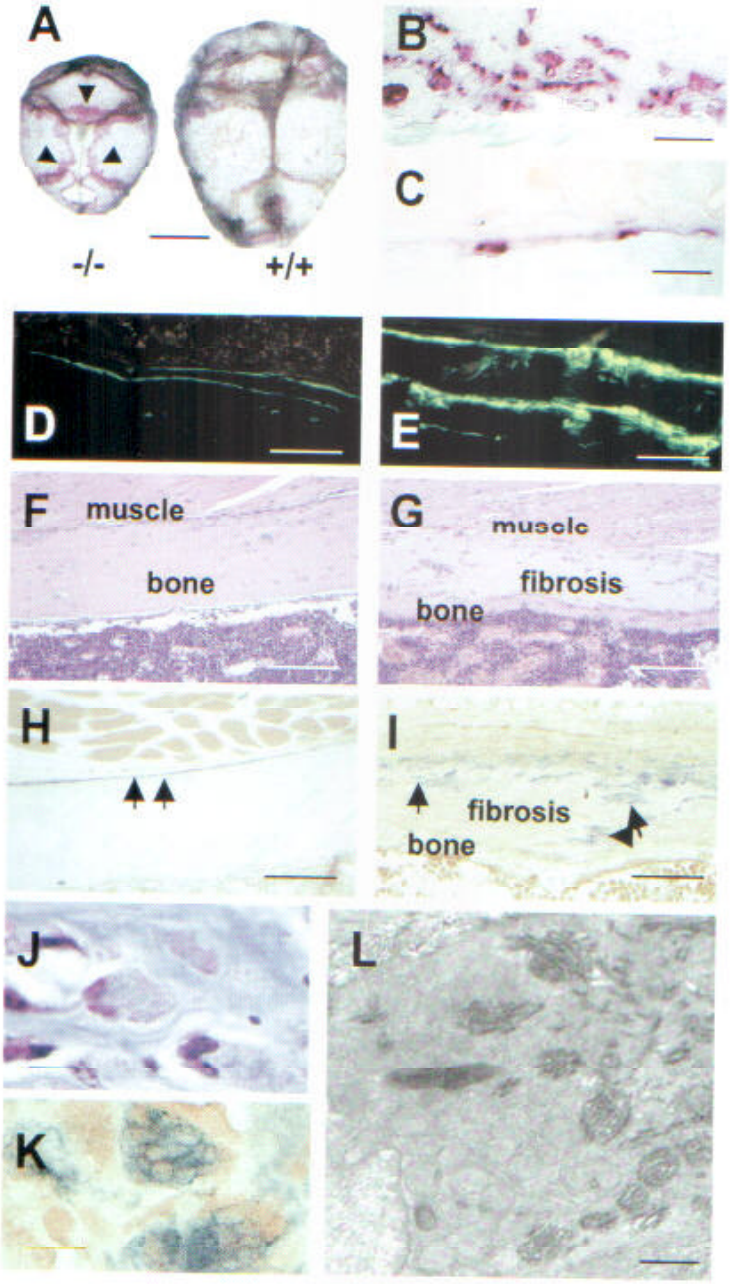

Figure 6. Bone Resorption and Formation in MT1-MMP-Deficient Mice

(A) TRAP staining of whole calvaria of 68-day-old mutant (−/−) and normal (+/+) littermates. The TRAP staining results in "painting" of the patent sutures in the mutant (arrowheads), indicating osteoclastic activity. (B and C) TRAP staining of the femoral cortex (metaphysis) in 68-day-old mutant (B) and wild-type (C) littermates (Nomarski optics). Note the large excess of osteoclasts in (B). (D and E) Calcein labeling of 69-day-old mice, tibial metaphysis. Mutant animals display a dramatic reduction in bone forming activity (D) compared to the wild type littermate (E). (F–I) Sections of femur of 51-day-old normal mouse (F and H) and mutant littermate (G and I), stained with H&E (F and G), and reacted for ALP (H and I) to demonstrate osteogenic cells (arrows). In the mutant, the cortical bone is markedly reduced in thickness and is lined by a thick fibrotic layer. ALP-positive cells are dispersed across the fibrotic layer (I, arrows). (J–L) Osteoblasts of the fibrotic periosteum of older animals contain intracellular collagen fibrils. (J), Trichrome strain. (K), ALP activity and (L), EM. Bars = 2.1 mm (A); 180 μm (B–E); 200 μm (F–I); 10 μm (J and K); 1.5 μm (L).

defects: impairment of osteogenic capacity and impairment of collagenolytic/gelatinolytic activity.

MT1-MMP-Deficient Skin Fibroblasts Are Incapable of Degrading Type I Collagen Matrices In Vitro

Because of the apparent inability of MT1-MMP-deficient marrow stromal cells to degrade the collagenous Gelfoam matrix, we sought to verify that MT1-MMP-deficient cells were deficient in collagenolytic activity. Skin fibroblasts isolated from newborn mice were seeded in a pellet on a reconstituted type I collagen fibril film and incubated in serum-free medium. Cells derived from wild-type or heterozygous mice readily degraded the underlying collagen film particularly when stimulated with TNFα/IL-1β. Cells from MT1-MMP-deficient littermates, however, completely failed to degrade the collagen matrix demonstrating that MT1-MMP deficiency imparts a severe defect in collagenolytic activity and that degradation of type I collagen fibrils in this system is absolutely dependent on MT1-MMP (Figure 7B).

Discussion

Targeted disruption of the *MT1-MMP* gene in mice results in a series of severe connective tissue growth and remodeling disorders including dwarfism, osteopenia, fibrosis of soft tissues, arthritis, and skeletal dysplasia.

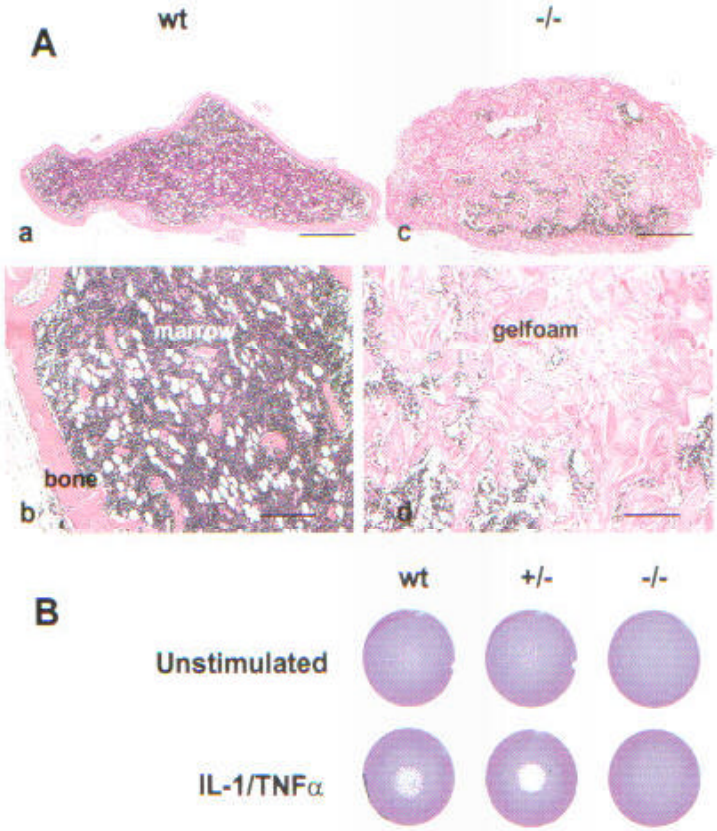

Figure 7. Osteogenesis and Collagen Breakdown by MT1-MMP-Deficient and Wild-Type Cells

(A) Function of osteogenic progenitor cells evaluated by their ability to form ectopic ossicles following transplantation in a collagen-based carrier in SCID mice. (a) Low-power view of the ossicle formed by cells derived from control animals. Note the well-developed bone cortex and marrow cavity with trabecular bone. (c) Low-power magnification of an ossicle formed by cells derived from MT1-MMP-deficient mice. Note the absence of cortical bone and little evidence of a marrow cavity. (b) High power view of the ossicle in (a) showing hematopoiesis, trabecular bone and adipocytes. (d) High power view of the ossicle in (c). Note the large amount of undegraded carrier. Bars = 0.8 mm (a and c); 250 μm (b and d).

(B) Collagenolytic activity of newborn skin fibroblasts seeded on a reconstituted type I collagen film. Note the failure of MT1-MMP-deficient to degrade the collagen film.

inability to degrade and remodel unmineralized collagenous matrices at sites that normally express MT1-MMP in the developing mouse emerges as a common denominator for these abnormalities. Consistent with these observations, cells derived from MT1-MMP-deficient animals have lost an indispensable collagenolytic activity against type I/II collagen-rich matrices. Our findings thus illustrate the pivotal and indispensable role of this collagenolytic activity in stromal remodeling and in the development, growth, and maintenance of connective tissue structures throughout the body.

Impaired Remodeling of Periskeletal Soft Tissues Gives Rise to Compensatory Osteoclastic Bone Resorption to Accommodate Growth

The skeleton is a major target for adverse effects of MT1-MMP deficiency (reduced longitudinal growth, cranial dysmorphism, osteoclasia, and osteopenia). None of these effects, however, reflect any detectable impairment of the osteoclast-mediated degradation of bone or calcified cartilage matrix. Rather, bone resorption and osteoclastic activity are greatly increased in MT1-MMP-deficient mice. This is in agreement with the notion that the collagenous-matrix-degrading activity of osteoclasts primarily is dependent on acidic proteinases of the cathepsin family (Garnero et al., 1998; Saftig et al., 1998), thus questioning MT1-MMP activity as essential for bone resorption. The progressive fibrosis of ligament, tendon and capsular insertions in bone suggests that timely remodeling of these soft tissue matrices was severely impaired to the extent that coordinated growth of the bone/soft tissue unit was compromised. As the soft tissues failed to remodel, the bone surface at the soft tissue insertion sites became a target for excessive osteoclastic bone resorption. Since bone is the only structure that can be efficiently remodeled in mutant animals, we propose that increased bone resorption vis-à-vis the development of soft tissue fibrosis constitutes a partially successful compensatory response enabling continued growth.

MT1-MMP Is Essential for Growth Plate Function and Secondary Ossification

Endochondral bone formation at metaphyseal growth plates involves coordinated removal of calcified cartilage by osteoclasts and subsequent replacement by bone deposited by osteoblasts. This process is essentially normal in MT1-MMP-deficient mice throughout prenatal development and even for some time after birth. We therefore conclude that the complex developmental program required for proper growth plate function (chondrocyte differentiation, maturation, hypertrophy, cartilage calcification, osteoclastic erosion), per se, is not dependent on MT1-MMP activity. The development of epiphyseal (secondary) centers of ossification, however, is disrupted in MT1-MMP-deficient mice. Invasion of the uncalcified epiphyseal hyaline cartilage by vascular canals which represents a critical early step in the development of the secondary centers of ossification

(Lutfi, 1970; Kuettner and Pauli, 1983; Cole and Wezeman, 1985) failed to occur. It is noteworthy that such vascular canals have previously been shown to express MT1-MMP (Ståhle-Bäckdahl et al., 1997). The formation of vascular canals involves degradation of uncalcified cartilage to clear a path for invading vessels that bring in osteogenic precursor cells for the ensuing ossification process. MT1-MMP plays a critical role in this angiogenic process although angiogenesis in general is not impaired in mutant mice. The failure to form vascular canals coincided with the onset of diminished longitudinal growth of long bones. The growth plates soon after showed progressive abnormalities including thinning, disorganization, and lack of chondrocyte proliferation. Considering their normal appearance prior to this time, we speculate that the delay of epiphyseal ossification may impair growth plate function. It has previously been suggested that mesenchymal cells which reach the interior of the epiphyseal cartilage by association with the blood vessels in vascular canals also serve as a reservoir of precursor cells for epiphyseal cartilage growth (Lutfi, 1970). If that is indeed the case, it is likely that the delay of epiphyseal vascularization results in a shortage of chondrocyte precursors and subsequent growth plate atrophy, as observed in MT1-MMP null mice.

MT1-MMP Deficiency Demonstrates the Fate and Function of Cartilage Primordia in Cranial Membranous Ossification

The craniofacial dysmorphology of MT1-MMP-deficient mice is particularly intriguing because it provides new insights into normal craniofacial development. The craniofacial abnormalities appear to be primarily associated with formation of membranous cranial bones and removal of their cartilage primordia. The role of these primordia is currently unclear, but they represent a prominent feature of embryonic cranial development in the mouse that has repeatedly been noted, but never fully explained (Ducy et al., 1997; Otto et al., 1997; Chen et al., 1998; Kaufmann, 1998). Membranous ossification of the parietal/interparietal bones proceeds through synchronous progression of bone formation and removal of the parietal cartilage so that the narrow overlapping boundary between the two moves gradually and continuously from the top toward the base of the skull. The developing bone forms outside the cartilage primordium and not within it as is the case in endochondral ossification. Our findings have shown that these cartilage primordia do not calcify and are not removed by osteoclasts, but rather by an entirely different directional chondrolytic process that is highly coordinated with the progression of bone formation. This chondrolytic process is specifically impaired in MT1-MMP-deficient mice. Consequently, an uncalcified, fibrous remnant of the calvarial cartilaginous primordium remains "inside" the cranial bones far into adulthood. It is interesting to note that underdevelopment of calvarial cartilage primordia in the *Imx1b* mutant mouse is associated with premature closure of cranial sutures (Chen et al., 1998), whereas in MT1-MMP-deficient mice failure to remove the cartilage primordia results in permanently open sutures. We note that all dysmorphic cranial bones in the MT1-MMP-deficient mice (orbital portions of frontal bones, parietal and interparietal bones) develop by membranous ossification but are preceded by conspicuous cartilage primordia (Kaufmann, 1998). Taken together, these findings suggest that development and timely removal of cartilage primordia are critical steps in cranial morphogenesis and suture formation. It is also interesting to note that facial features similar to those of the MT1-MMP-deficient mouse have been reported previously in a mouse mutation, *pn* (Kidwell et al., 1961), with the same chromosomal location as *mt1-mmp* (Apte et al., 1997). Unfortunately, this mouse strain is no longer available.

Remodeling of Unmineralized Connective Tissue Is Essential for Bone Formation

We have demonstrated that the function of bone-forming cells is severely impaired by MT1-MMP deficiency. This defect is coincident with signs of severe disorganization and disruption in the osteogenic periosteum. Transplantation of osteogenic cells to MT1-MMP-sufficient hosts confirmed that MT1-MMP deficiency caused an intrinsic defect of osteogenic cells that could not be rescued by an MT1-MMP-sufficient environment. The transplantation experiment also showed that the defect in osteogenesis is coupled to inability to degrade a collagenous matrix, a finding that is consistent with extensive fibrosis of the osteogenic periosteum and disruption of its highly ordered cellular architecture. The unusual finding of collagen fibrils inside osteoblasts, moreover, suggested that these cells attempted to mobilize a compensatory phagocytic pathway of collagen degradation (Melcher and Chan, 1981). We therefore speculate that inability to remodel the surrounding collagenous matrix may result in disorganization of the osteoblast layer, displacement of osteoblasts, and failure to achieve a level of coordinated function required for bone formation.

MT1-MMP Deficiency Gives Rise to Arthritis

The development of severe arthritis in aging MT1-MMP-deficient mice is particularly noteworthy in view of the many reports in the literature of overexpression of individual MMPs in human arthritis (Ståhle-Bäckdahl et al., 1997; Johnson et al., 1998). This observation should be carefully considered before employing MMP inhibitors in arthritis therapy. The arthritis that develops in MT1-MMP-deficient mice bears some resemblance to both murine collagen-induced arthritis and human rheumatoid arthritis; one noted element of similarity being the development of TRAP-positive osteoclast-like cells in articular and periarticular soft tissues (Gravallese et al., 1998; Suzuki et al., 1998). Although our experiments have not addressed the pathogenesis of arthritis in MT1-MMP-deficient mice, we note that interfaces between bone/cartilage and articular soft tissues are most severely affected. These are also sites where MT1-MMP is expressed at particularly high levels (Apte et al., 1997). In the knee for example, the insertion of the cruciate ligament where ligament, bone, and articular cartilage interface was most profoundly affected. These observations raise the question whether the arthritic changes in MT1-MMP-deficient mice develop as a result of inappropriate remodeling during growth.

MT1-MMP Mediates Pericellular Collagenolysis and Is Indispensable for Development and Growth

Our findings have shown that MT1-MMP is indispensable for growth and development and that lack of this enzyme cannot be adequately compensated by other membrane-associated MMPs, by other MMPs or by other collagen degrading mechanisms. MT1-MMP has been implicated as a possible activator of MMP-2 and MMP-13 (Strongin et al., 1995; Cowell et al., 1998), and MT1-MMP is sometimes, but not always coexpressed with either MMP-2 or MMP-13 in mice (Gack et al., 1995; Mattot et al., 1995; Kinoh et al., 1996; Apte et al., 1997). MMP-2-deficient mice, however, display a rather subtle phenotype that appears to have little, if anything, in common with the MT1-MMP phenotype (Itoh et al., 1997), thus all but dispelling the hypothesis that the MT1-MMP-deficient phenotype is primarily caused by failure to activate MMP-2. Moreover, MT1-MMP and MMP-13 are not coexpressed in embryonic tissues such as tendon, which later become profoundly affected in MT1-MMP-deficient mice. We therefore surmise that the effects of MT1-MMP deficiency, at least in the mouse, may not exclusively be mediated by lack of activation of MMP-13. At the cellular level, however, MT1-MMP deficiency does lead to the loss of an indispensable collagenolytic activity. Based on these observations and on existing evidence that MT1-MMP is capable of cleaving extracellular matrix substrates such as collagen and fibrin (Ohuchi et al., 1997; Hiraoka et al., 1998), we raise the question whether MT1-MMP functions as a collagenase in its own right or through activation of known or yet unrecognized type I/type II collagen-degrading proteinases. Regardless, loss of MT1-MMP-directed proteolysis results in profound and far reaching physiological consequences. Equally significant, the phenotype illustrates the importance of collagenous stromal remodeling for development and growth, and for maintenance of the otherwise invisible functional continuity between the soft and hard tissue components of the skeleton.

Experimental Procedures

All procedures were performed in accordance with an institutionally approved protocol for the use of animals in research.

Construction of Targeting Vector and Generation of Transgenic Mice

The MT1-MMP replacement type targeting vector was constructed using gene sequences cloned from a 129 strain mouse genomic library in the Lambda Fix II vector (Stratagene, La Jolla, CA). The targeting vector cloned into pBluescript SK$^-$ included a 4.9 kb 5′ homology spanning sequences from BglII site in the proximal promoter to the XbaI site in the middle part of intron 1. The 1.3 kb 3′ homology encompassed sequences from the PvuI site in exon 5 to the KpnI site in exon 8. Sequences from the XbaI site in intron 1 through the PvuI site in exon 5 were replaced with a phosphoglycerate kinase promoter–driven HPRT minigene EcoRI cassette (van der Lugt et al., 1991). The targeting vector was completed by addition of an HSV-tk minigene cloned into the KpnI site in the 3′ terminus of the short homology and the KpnI site of the plasmid polylinker.

HM-1 mouse ES cells (Magin et al., 1992) were transfected with the targeting vector and subjected to selection in growth medium supplemented with 0.1 mM hypoxanthine, 16 μM thymidine, 0.4 μM aminopterin (HAT supplement, GIBCO-BRL, Gaithersburg, MD), and 2 μM ganciclovir (Roche Laboratories, Nutley, NJ).

HAT-resistant clones were expanded and screened for the legitimate targeting event using a primer complementary to the HPRT minigene p01: 5′ GTG CGA GGC CAG AGG CCA CTT GTG TAG CG 3′; and a primer complementary to sequences not included in the targeting vector p02: 5′ GAA GAA GTA GGT CTT CCC ATT GGG CAT 3′. Cell clones containing the targeted allele were further characterized by Southern blot analysis. For analysis of the 3′ end of the targeted gene, DNA was restricted with HindIII, gel fractionated, and hybridized to a 495 bp PCR-generated cDNA probe spanning all of exons 6 through 8. For analysis of the 5′ end of the targeted gene, DNA was restricted with HindIII/BglII, gel fractionated, and hybridized to an 80 bp SstII probe spanning exon 1.

To generate chimeric mice, targeted ES cells were injected into 72 hr–old blastocysts from C57BL/6 mice and implanted into pseudopregnant B6D2 or C57BL/6 × DBA females (NCI–Frederick, Frederick, MD). Offspring were mated to Black Swiss mice (Taconic, Germantown, NY) to generate heterozygous animals for the targeted gene. These were subsequently interbred to generate homozygous mutant progeny.

Genotyping of animals was performed by PCR amplification of DNA obtained from tail biopsies with primers p01: 5′ GTG CGA GGC CAG AGG CCA CTT GTG TAG CG 3′ and p03: 5′CTT TGT GGG TGA CCC TGA CTT GC 3′ to detect the targeted allele; and primers p04: 5′ CTA GGC CTG GAA CAT TCT AAC GAT C 3′ and p03: 5′CTT TGT GGG TGA CCC TGA CTT GC 3′ to detect the wild-type allele.

Preparation of RNA

Total RNA was prepared by snap freezing tissue in liquid N_2 followed by extraction in Trizol (GIBCO-BRL, Gaithersburg, MD). Twenty-microgram samples of total RNA were size fractionated on formaldehyde agarose gels, immobilized on nylon membranes, and hybridized to the radiolabeled probes used for Southern blot analysis.

X-Ray Imaging

X-ray imaging of animals was performed in a Faxitron MX-20 X-ray machine (Faxitron X-ray Corp., Buffalo Grove, IL).

In Vivo Labeling

Calcein (25 mg/kg bodyweight in 2% $NaHCO_3$) was injected i.p. at day 0 and 10 days later. Tissues were harvested at day 12 and fixed in 70% ethanol. Bones were processed for methyl-methacrylate embedding and 10 μm sections were analyzed by fluorescence microscopy in a Zeiss Axiophot. BrdU labeling was performed as described (Vu et al., 1998).

Histology and Microscopy

Tissues were fixed in neutral buffered formalin, decalcified in formic acid or EDTA, paraffin embedded, sectioned at 6 μm, and stained with H&E, Masson's trichrome, PAS stain, or alcian blue. Additional samples of long bones were fixed embedded undecalcified in glycol-methacrylate (GMA) at low temperature or in methyl-methacrylate (MMA). Two-to-four μm–thick GMA sections were reacted for TRAP or ALP activity as described (Bianco et al., 1984). MMA sections were stained with Goldner's or von Kossa's stains. Entire calvaria were fixed in 70% ethanol for 5 min and reacted for TRAP and ALP using Sigma (St. Louis, MO) kits. Alcian blue/alizarin red stain was performed as described (Kaufmann, 1998). For EM, mice were perfusion fixed with 2% paraformaldehyde/2% glutaraldehyde in 0.1 M cacodylate buffer, pH 7.4. Samples were decalcified in 0.1 M EDTA in 0.15 M phosphate buffer, postfixed in 1% OsO_4, and embedded in Spurr's medium. Thin sections were photographed in a JEOL 100 CXII electron microscope.

In Vivo Assay of Osteogenic Capacity of Bone Marrow–Derived Stromal Cells from Normal and Transgenic Mice

Osteogenic precursor cells (bone marrow stromal cells) were derived from the bone marrow of 2-month-old mice as described (Kuznetsov and Gehron Robey, 1996). Confluent cultures were passaged 3 times, and 2.4 × 10^6 BMCSs were mixed with denatured type I collagen sponges (25–50 mm^2, Gelfoam, Upjohn, Kalamazoo, MI) or hydroxyapatite-tricalcium phosphate ceramic particles (40 mg of particles, Zimmer, Warsaw, IN) and transplanted to the subcutis

of immunocompromised (NIH bg nu xidBR) mice (Harlan Sprague Dawley, Indianapolis, IN). Ossicles were harvested for histology at 8 weeks as described (Krebsbach et al., 1997).

Collagen Degradation Assay

The capacity of cells to degrade type I collagen fibrils was assessed as described (Havemose-Poulsen et al., 1998). Briefly, 24-well plates were coated with a 1–2 μm film of reconstituted rat tail tendon type I collagen fibrils, and a pellet of 37,500 cells in 25 μl growth medium (DMEM, 10% [v/v] FBS) was seeded in the center of each well. Newborn skin fibroblasts were allowed to attach for 5 hr, washed 3 times in HBSS, and then incubated for 5 days in serum free Opti-MEM I (GIBCO-BRL, Gaithersburg, MD) with or without addition of 10^{-9} M IL-1β and 10^{-8} M TNFα. Following incubation, cells were removed with trypsin/EDTA and the residual collagen fibril film stained with Coomassie blue.

Acknowledgments

We thank Anna-Maria Spliid, and the NIDCR Animal Care Unit for invaluable help with husbandry and record keeping, the NIDCR Gene Targeting Facility and Glenn Longenecker for blastocyst injections and implantation, and Bill Swaim for EM imaging. This work was supported in part with fellowships for K. H. from the Danish Cancer Society and the Danish Medical Research Council.

Received May 14, 1999; revised August 27, 1999.

References

Apte, S.S., Fukai, N., Beier, D.R., and Olsen, B.R. (1997). The matrix metalloproteinase-14 (MMP-14) gene is structurally distinct from other MMP genes and is co-expressed with the TIMP-2 gene during mouse embryogenesis. J. Biol. Chem. *272*, 25511–25517.

Bianco, P., Ponzi, A., and Bonucci, E. (1984). Basic and 'special' stains for plastic sections in bone marrow histopathology, with special reference to May-Grunwald Giemsa and enzyme histochemistry. Basic Appl. Histochem. *28*, 265–279.

Birkedal-Hansen, H. (1995). Proteolytic remodeling of extracellular matrix. Curr. Opin. Cell. Biol. *7*, 728–735.

Birkedal-Hansen, H., Moore, H., Bodden, M.K., Windsor, L.J., Birkedal-Hansen, B., De Carlo, A., and Engler, J.A. (1993). Matrix metalloproteinases: a review. Crit. Rev. Oral Biol. Med. *4*, 197–250.

Chen, H., Ovchinnikov, D., Pressman, C.L., Aulehla, A., Lun, Y., and Johnson, R.L. (1998). Multiple calvarial defects in lmx1b mutant mice. Dev. Genet. *22*, 314–320.

Chin, J.R., and Werb, Z. (1997). Matrix metalloproteinases regulate morphogenesis, migration and remodeling of epithelium, tongue skeletal muscle and cartilage in the mandibular arch. Development *124*, 1519–1530.

Cole, A.A., and Wezeman, F.H. (1985). Perivascular cells in cartilage canals of the developing mouse epiphysis. Am. J. Anat. *174*, 119–129.

Cowell, S., Knauper, V., Stewart, M.L., D'Ortho, M.P., Stanton, H., Hembry, R.M., Lopez-Otin, C., Reynolds, J.J., and Murphy, G. (1998). Induction of matrix metalloproteinase activation cascades based on membrane-type 1 matrix metalloproteinase: associated activation of gelatinase A, gelatinase B and collagenase 3. Biochem. J. *331*, 453–458.

Ducy, P., Zhang, R., Geoffroy, V., Ridall, A.L., and Karsenty, G. (1997). Osf2/Cbfa1: a transcriptional activator of osteoblast differentiation. Cell *89*, 747–754.

Gack, S., Vallon, R., Schmidt, J., Grigoriadis, A., Tuckermann, J., Schenkel, J., Weiher, H., Wagner, E.F., and Angel, P. (1995). Expression of interstitial collagenase during skeletal development of the mouse is restricted to osteoblast-like cells and hypertrophic chondrocytes. Cell Growth. Differ. *6*, 759–767.

Galis, Z.S., Sukhova, G.K., Kranzhofer, R., Clark, S., and Libby, P. (1995). Macrophage foam cells from experimental atheroma constitutively produce matrix-degrading proteinases. Proc. Natl. Acad. Sci. USA *92*, 402–406.

Gamero, P., Borel, O., Byrjalsen, I., Ferreras, M., Drake, F.H., McQueney, M.S., Foged, N.T., Delmas, P.D., and Delaisse, J.M. (1998). The collagenolytic activity of cathepsin K is unique among mammalian proteinases. J. Biol. Chem. *273*, 32347–32352.

Gravallese, E.M., Harada, Y., Wang, J.T., Gorn, A.H., Thornhill, T.S., and Goldring, S.R. (1998). Identification of cell types responsible for bone resorption in rheumatoid arthritis and juvenile rheumatoid arthritis. Am. J. Pathol. *152*, 943–951.

Havemose-Poulsen, A., Holmstrup, P., Stoltze, K., and Birkedal-Hansen, H. (1998). Dissolution of type I collagen fibrils by gingival fibroblasts isolated from patients of various periodontitis categories. J. Periodontal Res. *33*, 280–291.

Hiraoka, N., Allen, E., Apel, I.J., Gyetko, M.R., and Weiss, S.J. (1998). Matrix metalloproteinases regulate neovascularization by acting as pericellular fibrinolysins. Cell *95*, 365–377.

Itoh, T., Ikeda, T., Gomi, H., Nakao, S., Suzuki, T., and Itohara, S. (1997). Unaltered secretion of beta-amyloid precursor protein in gelatinase A (matrix metalloproteinase 2)-deficient mice. J. Biol. Chem. *272*, 22389–22392.

Johnson, L.L., Dyer, R., and Hupe, D.J. (1998). Matrix metalloproteinases. Curr. Opin. Chem. Biol. *2*, 466–471.

Kaufmann, M.H. (1998). The Atlas of Mouse Development, Revised Edition (San Diego: Academic Press).

Kidwell, J.F., Gowen, J.W., and Stadler, J. (1961). Pugnose—a recessive mutation in linkage group 3 of mice. J. Hered. *52*, 145–148.

Kinoh, H., Sato, H., Tsunezuka, Y., Takino, T., Kawashima, A., Okada, Y., and Seiki, M. (1996). MT-MMP, the cell surface activator of proMMP-2 (pro-gelatinase A), is expressed with its substrate in mouse tissue during embryogenesis. J. Cell. Sci. *109*, 953–959.

Krebsbach, P.H., Kuznetsov, S.A., Satomura, K., Emmons, R.V., Rowe, D.W., and Gehron Robey, P. (1997). Bone formation in vivo: comparison of osteogenesis by transplanted mouse and human marrow stromal fibroblasts. Transplantation *63*, 1059–1069.

Kuettner, K.E., and Pauli, B.U. (1983). Vascularity of cartilage. In Cartilage, B.K. Hall, ed. (New York: Academic Press), pp. 281–312.

Kuznetsov, S., and Gehron Robey, P. (1996). Species differences in growth requirements for bone marrow stromal fibroblast colony formation in vitro. Calcif. Tissue Int. *59*, 265–270.

Lark, M.W., Bayne, E.K., Flanagan, J., Harper, C.F., Hoerrner, L.A., Hutchinson, N.I., Singer, I.I., Donatelli, S.A., Weidner, J.R., Williams, H.R., Mumford, R.A., and Lohmander, L.S. (1997). Aggrecan degradation in human cartilage. Evidence for both matrix metalloproteinase and aggrecanase activity in normal, osteoarthritic, and rheumatoid joints. J. Clin. Invest. *100*, 93–106.

Liotta, L.A., Steeg, P.S., and Stetler-Stevenson, W.G. (1991). Cancer metastasis and angiogenesis: an imbalance of positive and negative regulation. Cell *64*, 327–336.

Lutfi, A.M. (1970). Mode of growth, fate and function of cartilage canals. J. Anat. *106*, 135–145.

Magin, T.M., McWhir, J., and Melton, D.W. (1992). A new mouse embryonic stem cell line with good germ line contribution and gene targeting frequency. Nucleic Acids Res. *20*, 3795–3796.

Masson, R., Lefebvre, O., Noel, A., Fahime, M.E., Chenard, M.P., Wendling, C., Kebers, F., LeMeur, M., Dierich, A., Foidart, J.M., et al. (1998). In vivo evidence that the stromelysin-3 metalloproteinase contributes in a paracrine manner to epithelial cell malignancy. J. Cell Biol. *140*, 1535–1541.

Mattot, V., Raes, M.B., Henriet, P., Eeckhout, Y., Stehelin, D., Vandenbunder, B., and Desbiens, X. (1995). Expression of interstitial collagenase is restricted to skeletal tissue during mouse embryogenesis. J. Cell. Sci. *108*, 529–535.

Melcher, A.H., and Chan, J. (1981). Phagocytosis and digestion of collagen by gingival fibroblasts in vivo: a study of serial sections. J. Ultrastruct. Res. *77*, 1–36.

Mignatti, P., and Rifkin, D.B. (1996). Plasminogen activators and matrix metalloproteinases in angiogenesis. Enzyme Protein *49*, 117–137.

Mudgett, J.S., Hutchinson, N.I., Chartrain, N.A., Forsyth, A.J., McDonnell, J., Singer, I.I., Bayne, E.K., Flanagan, J., Kawka, D., Shen, C.F., Stevens, K., Chen, H., Trumbauer, M., and Visco, D.M.

(1998). Susceptibility of stromelysin 1-deficient mice to collagen induced arthritis and cartilage destruction. Arthritis Rheum. *41*, 110–121.

Nagase, H. (1998). Cell surface activation of progelatinase A (proMMP-2) and cell migration. Cell Res. *8*, 179–186.

Ohuchi, E., Imai, K., Fujii, Y., Sato, H., Seiki, M., and Okada, Y. (1997). Membrane type 1 matrix metalloproteinase digests interstitial collagens and other extracellular matrix macromolecules. J. Biol. Chem. *272*. 2446–2451.

Okada, A., Tomasetto, C., Lutz, Y., Bellocq, J.P., Rio, M.C., and Basset, P. (1997). Expression of matrix metalloproteinases during rat skin wound healing: evidence that membrane type-1 matrix metalloproteinase is a stromal activator of pro-gelatinase A. J. Cell Biol. *137*, 67–77.

Otto, F., Thornell, A.P., Crompton, T., Denzel, A., Gilmour, K.C., Rosewell, I.R., Stamp, G.W., Beddington, R.S., Mundlos, S., Olsen, B.R., et al. (1997). Cbfa1, a candidate gene for cleidocranial dysplasia syndrome, is essential for osteoblast differentiation and bone development. Cell *89*, 765–771.

Pei, D. (1999). Identification and characterization of the fifth membrane-type matrix metalloproteinase MT5-MMP. J. Biol. Chem. *274*, 8925–8932.

Puente, X.S., Pendas, A.M., Llano, E., Velasco, G., and Lopez-Otin, C. (1996). Molecular cloning of a novel membrane-type matrix metalloproteinase from a human breast carcinoma. Cancer Res. *56*, 944–949.

Saftig, P., Hunziker, E., Wehmeyer, O., Jones, S., Boyde, A., Rommerskirch, W., Moritz, J.D., Schu, P., and von Figura, K. (1998). Impaired osteoclastic bone resorption leads to osteopetrosis in cathepsin-K-deficient mice. Proc. Natl. Acad. Sci. USA *95*, 13453–13458.

Sato, H., Takino, T., Okada, Y., Cao, J., Shinagawa, A., Yamamoto, E., and Seiki, M. (1994). A matrix metalloproteinase expressed on the surface of invasive tumour cells. Nature *370*, 61–55.

Sato, H., Kinoshita, T., Takino, T., Nakayama, K., and Seiki, M. (1996). Activation of a recombinant membrane type 1-matrix metalloproteinase (MT1-MMP) by furin and its interaction with tissue inhibitor of metalloproteinases (TIMP)-2. FEBS Lett. *393*, 101–104.

Shipley, J.M., Wesselschmidt, R.L., Kobayashi, D.K., Ley, T.J., and Shapiro, S.D. (1996). Metalloelastase is required for macrophage-mediated proteolysis and matrix invasion in mice. Proc. Natl. Acad. Sci. USA *93*, 3942–3946.

Ståhle-Bäckdahl, M., Sandstedt, B., Bruce, K., Lindahl, A., Jimenez, M.G., Vega, J.A., and Lopez-Otin, C. (1997). Collagenase-3 (MMP-13) is expressed during human fetal ossification and re-expressed in post-natal bone remodeling and in rheumatoid arthritis. Lab. Invest. *76*, 717–728.

Stetler-Stevenson, W.G., Aznavoorian, S., and Liotta, L.A. (1993). Tumor cell interactions with the extracellular matrix during invasion and metastasis. Annu. Rev. Cell Biol. *9*, 541–573.

Strongin, A.Y., Collier, I., Bannikov, G., Marmer, B.L., Grant, G.A., and Goldberg, G.I. (1995). Mechanism of cell surface activation of 72-kDa type IV collagenase. Isolation of the activated form of the membrane metalloprotease. J. Biol. Chem. *270*, 5331–5338.

Suzuki, Y., Nishikaku, F., Nakatuka, M., and Koga, Y. (1998). Osteoclast-like cells in murine collagen induced arthritis. J. Rheumatol. *25*, 1154–1160.

Takino, T., Sato, H., Shinagawa, A., and Seiki, M. (1995). Identification of the second membrane-type matrix metalloproteinase (MT-MMP-2) gene from a human placenta cDNA library. MT-MMPs form a unique membrane-type subclass in the MMP family. J. Biol. Chem. *270*, 23013–23020.

van der Lugt, N., Maandag, E.R., te Riele, H., Laird, P.W., and Berns, A. (1991). A pgk/hprt fusion as a selectable marker for targeting of genes in mouse embryonic stem cells: disruption of the T-cell receptor delta-chain-encoding gene. Gene *105*, 263–267.

Vu, T.H., Shipley, J.M., Bergers, G., Berger, J.E., Helms, J.A., Hanahan, D., Shapiro, S.D., Senior, R.M., and Werb, Z. (1998). MMP-9/gelatinase B is a key regulator of growth plate angiogenesis and apoptosis of hypertrophic chondrocytes. Cell *93*, 411–422.

Werb, Z. (1997). ECM and cell surface proteolysis: regulating cellular ecology. Cell *91*, 439–442.

Werb, Z., Sympson, C.J., Alexander, C.M., Thomasset, N., Lund, L.R., MacAuley, A., Ashkenas, J., and Bissell, M.J. (1996). Extracellular matrix remodeling and the regulation of epithelial- stromal interactions during differentiation and involution. Kidney Int. Suppl. *54*, S68–74.

Will, H., and Hinzmann, B. (1995). cDNA sequence and mRNA tissue distribution of a novel human matrix metalloproteinase with a potential transmembrane segment. Eur. J. Biochem. *231*, 602–608.

Wilson, C.L., Heppner, K.J., Labosky, P.A., Hogan, B.L., and Matrisian, L.M. (1997). Intestinal tumorigenesis is suppressed in mice lacking the metalloproteinase matrilysin. Proc. Natl. Acad. Sci. USA *94*, 1402–1407.